

## Resistivity and Calibration Error Estimations for Small-Loop Electromagnetic Method

Yutaka Sasaki<sup>1)</sup>, Jeong-Sul Son<sup>2)</sup>, Changryol Kim<sup>2)</sup>, Jung-Ho Kim<sup>2)</sup>

<sup>1)</sup>Dept. of Earth Resource Engineering., Kyushu Univ., Japan, sasaki@mine.kyushu-u.ac.jp

<sup>2)</sup>Geotechnical Engineering Div., KIGAM, Korea

**Abstract:** The frequency-domain small-loop electromagnetic (EM) instruments are increasingly used for shallow environmental and geotechnical surveys because of their portability and speed. However, it is well known that the data quality is generally so poor that quantitative interpretation of the data is not justified in many cases. We present an inversion method that allows the correction for the calibration errors and also constructs multidimensional resistivity models. The key point in this method is that the data are collected at least at two different heights. The forward modeling used in the inversion is based on an efficient 3-D finite-difference method, and its solution was checked against 2-D finite-element solution. The synthetic and real data examples demonstrate that the joint inversion recovers reliable resistivity models from multi-frequency data severely contaminated by the calibration errors.

**Keywords:** electromagnetic method, small-loop EM, joint inversion, calibration errors

### 1. INTRODUCTION

Small-loop Electromagnetic (EM) method is emerging as an important tool for shallow environmental and geotechnical investigations. Its advantages are: (1) the portability and speed in field operation, (2) simultaneous acquisition of multiple frequency data, and (3) excellent lateral resolution. Interpretation of small-loop EM data is commonly based on mapping of apparent conductivity calculated from the measured magnetic field. However, for many applications, information on vertical variation in conductivity structure is demanded. Huang and Won (2003) argue that depth sounding by changing frequency is possible with their EM sensor, showing synthetic and field data examples of layered-model (1-D) inversion. However, it is well known that the quality of small-loop EM data is not good enough to do any quantitative interpretation. The small-loop EM system requires an accurately calibrated receiver to measure the secondary magnetic field in the presence of the dominant primary field. Even if an EM system is calibrated very precisely at a factory, the errors due to temporal change in the coil position are inevitable in the field. The recommended procedure for correcting the EM signal is to raise the sensor high above the ground (for instance, by hanging it to a tall tree) so that the sensor output approach zero (Won, 2003), However, this is not practical in common field situations.

In this paper, we propose a method for correcting for the calibration errors numerically and also inverting for 2-D (or 3-D) resistivity model at the same time. We demonstrate its effectiveness using synthetic and field data examples.

### 2. INVERSION METHOD

The subsurface is assumed to be divided into a set of rectangular blocks. Let the logarithms of the resistivities of the blocks be represented by the vector  $\mathbf{m}$  and let observed data be the vector

**d.** The data consist of the in-phase and quadrature components of the secondary magnetic field normalized by the (free-space) primary field, and are assumed to be collected at multiple heights above the ground. When considering calibration errors, the inverse problem can be written as

$$\mathbf{d} = \mathbf{f}(\mathbf{m}) + \mathbf{G}\mathbf{s}, \quad (1)$$

where  $\mathbf{f}(\mathbf{m})$  is the forward modeling function that generates the theoretical response for the model  $\mathbf{m}$ ,  $\mathbf{s}$  represents the calibration errors (or offset values) contained in the data, which are different for the in-phase and quadrature components for each frequency, and  $\mathbf{G}$  is a matrix that relates calibration errors to the data. The rows of  $\mathbf{G}$  have one at the appropriate locations. Note that the size of  $\mathbf{s}$  (or the number of the offset values) is equal to twice the number of the frequencies.

The solution of equation (1) is numerically unstable in the presence of noise. The inverse problem is therefore formulated as an optimization problem in which the solution is taken as a model that minimizes the objective function

$$\phi = \|\mathbf{W}[\mathbf{d} - \mathbf{f}(\mathbf{m}) - \mathbf{G}\mathbf{s}]\|^2 + \lambda^2 \|\mathbf{C}\mathbf{m}\|^2, \quad (2)$$

where  $\mathbf{W}$  is a diagonal matrix assigning weights to each datum,  $\mathbf{C}$  is a second-order finite-difference operator used to quantify the model roughness, and  $\lambda$  is a Lagrange multiplier. The optimization problem is iteratively solved by using a linearized approximation of the model function. Let  $\Delta\mathbf{m}^k$  be the perturbation at the  $k$ th iteration to the current model  $\mathbf{m}^{k-1}$ . The objective function is approximated by

$$\phi = \|\mathbf{W}[\Delta\mathbf{d} - \mathbf{A}\Delta\mathbf{m}^k - \mathbf{G}\mathbf{s}]\|^2 + \lambda^2 \|\mathbf{C}(\mathbf{m}^{k-1} + \Delta\mathbf{m}^k)\|^2, \quad (3)$$

where  $\mathbf{A}$  is the Jacobian matrix of sensitivities with respect to the model parameters, and

$$\Delta\mathbf{d} = \mathbf{d} - \mathbf{f}(\mathbf{m}^{k-1}) \quad (4)$$

is the vector of differences between the observed and predicted data. The minimization of  $\phi$  is equivalent to obtaining the least-squares solution of the rectangular system

$$\begin{bmatrix} \mathbf{W}\mathbf{A}\mathbf{W}\mathbf{G} \\ \lambda\mathbf{C} & 0 \end{bmatrix} \begin{Bmatrix} \Delta\mathbf{m}^k \\ \mathbf{s} \end{Bmatrix} = \begin{Bmatrix} \mathbf{W}\Delta\mathbf{d} \\ -\lambda\mathbf{C}\mathbf{m}^{k-1} \end{Bmatrix}. \quad (5)$$

We use the modified Gram-Schmidt method to solve equation (5). The new model is given by

$$\mathbf{m}^k = \mathbf{m}^{k-1} + \Delta\mathbf{m}^k. \quad (6)$$

The method described above is basically the same as the one used for multidimensional inversion of horizontal-loop EM data (Sasaki and Meju, 2006), except that offset values of the data are incorporated into the inversion process.

### 3. VERIFICATION OF FORWARD MODELING

The forward modeling used is based on an efficient finite-difference (FD) method in which the EM fields are solved on a 3-D staggered grid (Sasaki, 2001). Since the multidimensional forward modeling for small-loop EM survey is relatively new, the 3-D FD solutions were checked against the 2.5-D finite-element (FE) solutions for two 2-D models shown in Fig.1. For both models, the horizontal loops are assumed to be separated by 2 m and located at the ground surface. The reason for comparing the responses at the surface is that the 2.5-D FE code used can give the EM response only on the surface. The FD modeling employs a grid of 63 by 29 by 27 (including 13 air layer) in the  $x$ -,  $y$ -, and  $z$ -directions, with the smallest grid size of 1 m by 2 m by 1 m. The 2-D FE modeling was carried out on a grid of 189 by 66 (including 18 air layer) in  $x$ - and  $z$ -directions, with the smallest grid size of 25 cm by 25 cm. Fig. 2 shows the comparisons of the secondary magnetic fields plotted in parts per million (ppm) of the primary field at four frequencies (40, 20, 10, and 5 kHz). Despite the fact that the discretization used for

3-D FD modeling is relatively coarse, the agreement is generally good.

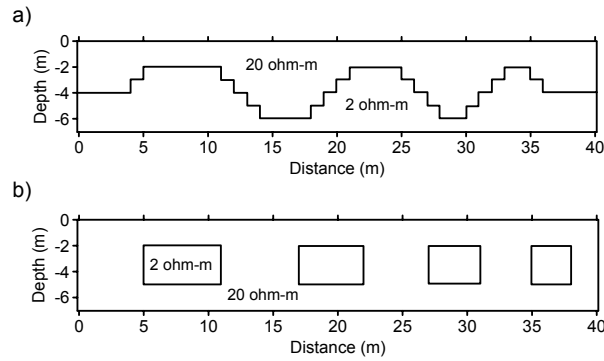


**Fig.1.** 2-D models used to verify the accuracy of the finite-difference solution for small-loop EM simulations.

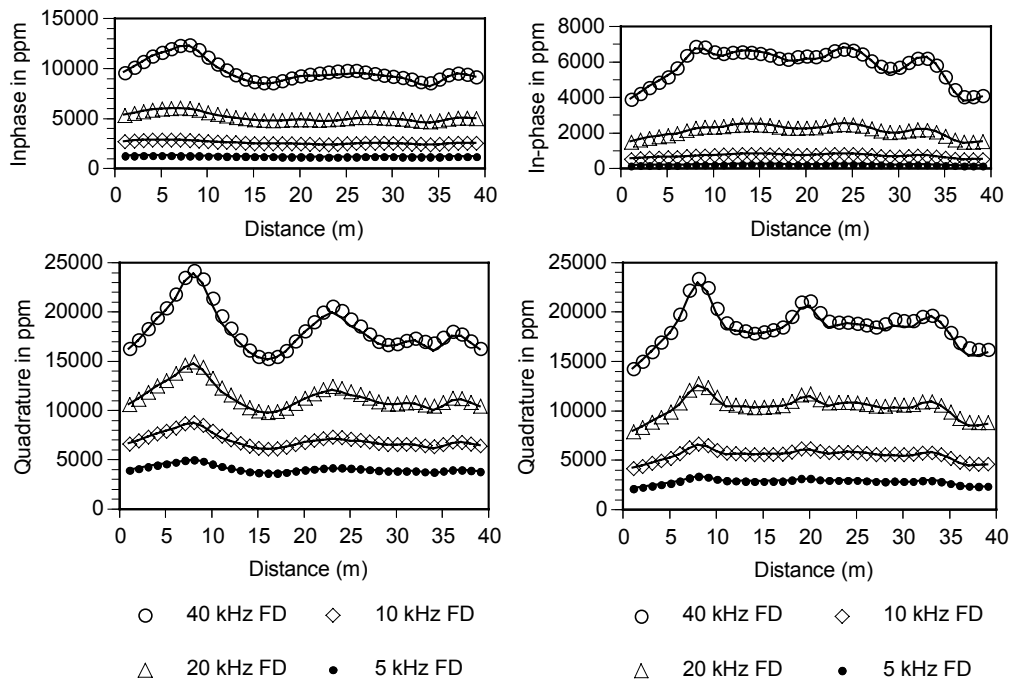


**Fig. 2.** Comparisons of the secondary magnetic field responses at the surface to Model 1 (left) and 2 (right), calculated using 3-D FD (symbols) and 2.5-D FE (solid lines) methods.

#### 4. SYNTHETIC EXAMPLE

We tested our joint inversion method on the data generated for the model shown in Fig.1a. The responses were computed at four frequencies (40, 20, 10, and 5 kHz) for 39 locations with an interval of 1 m, assuming a loop separation of 2 m and the height of the loops above the ground to be 1 and 2 m. The grid used is the same as before. The computed responses were contaminated with Gaussian noise, with a standard deviation of either 1 % of the magnitude of the datum or 100 ppm. In addition, the data were deliberately shifted by a constant value at each frequency to simulate calibration errors; the shifted values are shown in Table 1. In the inversion, the subsurface was divided into 280 (40 by 1 by 7) cells of unknown resistivity. The

model constructed from conventional 2-D inversion of a data set for a height of 1 m is shown in Fig. 3b. This resistivity image appears to be considerably distorted. The 2-D joint inversion for resistivities and calibration errors was applied to all the data for heights of 1 and 2 m. The inversions starting with homogeneous half-space models of resistivity 100 and 10 ohm-m produced the models shown in Fig. 3c and 3d, respectively. There are virtually no differences between the two inversion results, which suggests that the joint inversion results are not dependent on the starting model. The data misfit reaches 106 ppm at the fifth iteration for both cases (Fig.4a). The calibration errors are almost correctly estimated as shown in Table 1. This synthetic example clearly shows that the calibration errors can be accurately estimated by joint inversion if the profile data are acquired for at least two different heights.

**Table 1.** Offset values assigned at each frequency and those estimated by joint inversions.

Freq. (Hz)	In-phase (ppm)			Quadrature (ppm)		
	True	Case 1	Case2	True	Case1	Case2
40,000	-1500	-1501	-1501	-3000	-2790	-2795
20,000	1000	934	935	-2500	-2414	-2417
10,000	800	746	747	-850	-830	-831
5,000	500	446	447	1000	978	978

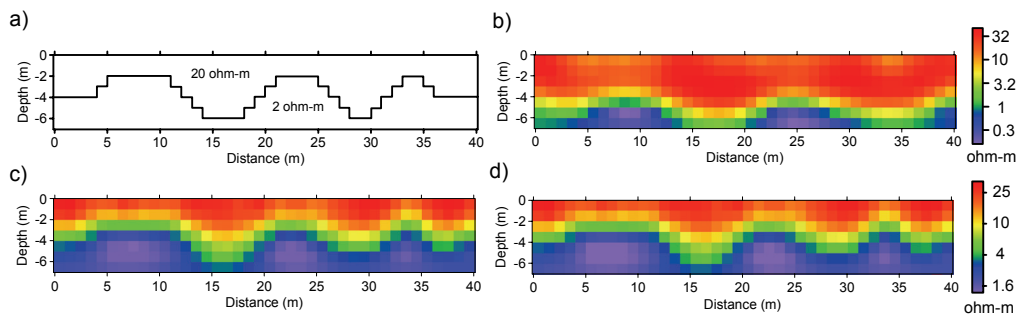


**Fig. 3.** 2-D test model (a) and corresponding inversion models obtained from a conventional inversion (b) and joint inversions using starting models of 100 (c) and 10 ohm-m half space (d)

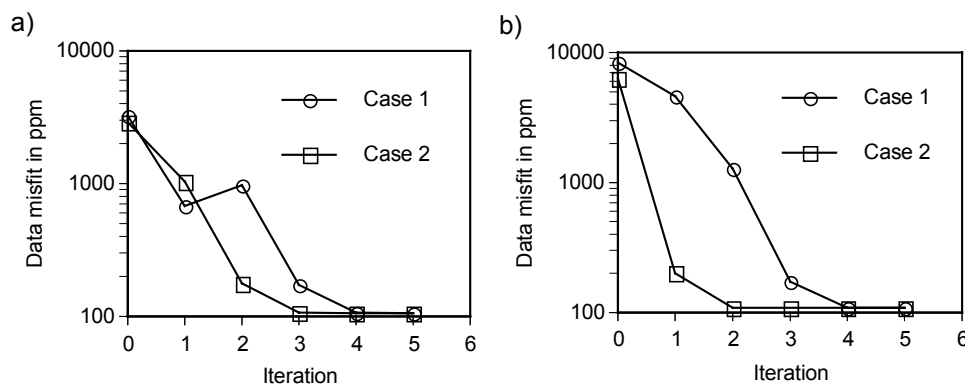


**Fig. 4.** Convergence for joint inversions of the synthetic data (a) and field data (b). Cases 1 and 2 refer to the inversion using 100 and 10 ohm-m half space as the starting model, respectively.

### 5. FIELD DATA EXAMPLE

In order to examine the applicability of the method to real data, a small-loop EM survey using GEM-2H was carried out in Yeonggwang coastal area, together with a dc resistivity survey. The EM data were collected along a 40-m survey line at two different heights, 0 m and 1 m above the ground. The dc resistivity data were taken along the same line using a dipole-dipole array, with a dipole length of 1 m and a maximum  $n$  spacing of 16. The resistivity structures recovered from 2-D inversions of EM and dc resistivity data are shown in Fig.5a and 5b, respectively. The starting model for EM inversion was a 100 ohm-m half space. We also tested a 10 ohm-m half space as the starting model and obtained a model (not shown) which was indistinguishable from the one in Fig.5a. The convergence in the form of data misfit versus iteration number is shown in Fig.4b for the two starting models. The final fits between the observed data that are corrected for calibration errors and the predicted data are shown in Fig.6. The estimated calibration errors are shown in Table 2. Note that most of the original in-phase data have quite large negative values, which is apparently caused by inadequate calibrations.

As a final experiment, we deliberately shifted the original field data by the same amount as in the synthetic example, and applied the joint inversions to the disturbed data using the same two starting models. The resulting models (not shown) were virtually the same as the one in Fig.5a again. This experiment gives us a confidence on the reliability of the joint inversion approach for interpreting EM data that are contaminated seriously by the inadequate calibrations.

**Table 2.** Offset values estimated by joint inversion of EM data taken in Yeonkwang coastal area. Cases 1 and 2 refer to inversion results obtained using 100 and 10 ohm-m starting models, respectively.

Freq. (Hz)	In-phase (ppm)		Quadrature (ppm)	
	Case 1	Case 2	Case 1	Case 2
40,110	-14263	-14292	12185	12226
19,350	-2627	-2651	3428	3438
9,330	-657	-672	1355	1353
4,530	-26	-34	519	514

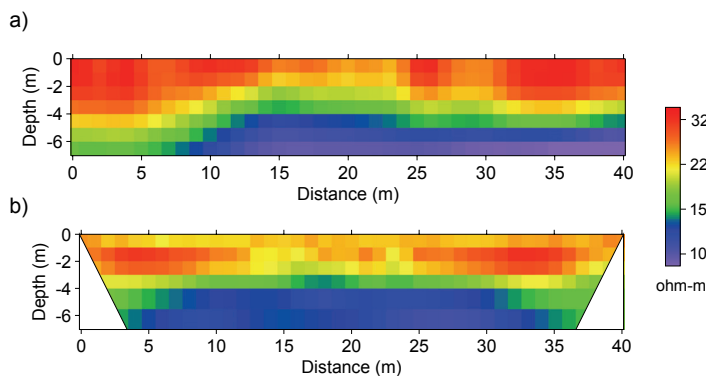


**Fig. 5.** Resistivity models constructed from 2-D inversion of EM data (a) and dipole-dipole data (b) in Yeonkwang coastal area.

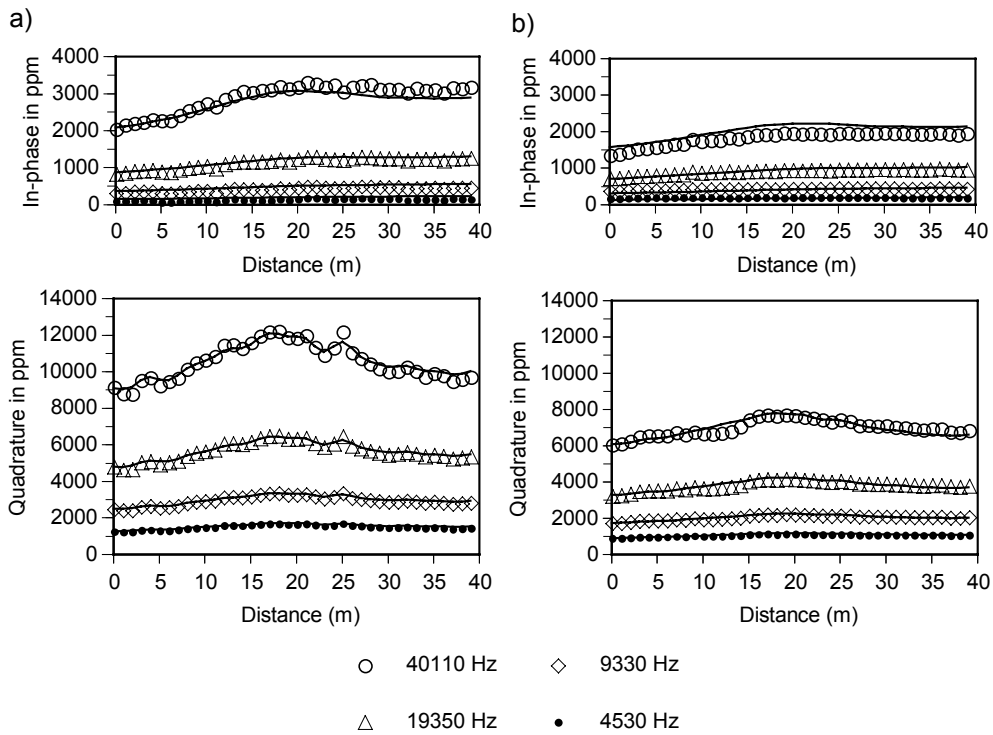


**Fig. 6.** Comparisons between the observations corrected for calibration errors (symbols) and the predicted data (lines). (a) Data collected at the surface. (b) Data collected at a height of 1 m.

## 6. CONCLUSIONS

We have proposed an inversion approach that enables us to obtain reliable multidimensional models even if the data are severely contaminated by calibration errors. The prerequisite for this method is to acquire the data at multiple heights. The synthetic and field data examples demonstrate that the inversion is stable and not dependent on the starting model and the amount of the calibration errors if the data are obtained at least at two different heights.

## ACKNOWLEDGMENTS

This research was supported by the Basic Research Project of the Korea Institute of Geoscience and Mineral Resources funded by the Ministry of Science and Technology of Korea.

## REFERENCES

- Huang, H. and Won, I.J., 2003, Real-time resistivity sounding using a hand-held broadband electromagnetic sensor, *Geophysics*, **68**, 1224-1231.
- Sasaki, Y., 2001, Full 3-D inversion of electromagnetic data on PC, *J. Applied Geophys.*, **46**, 45-54.
- Sasaki, Y. and Meju, M.A., 2006, A multidimensional horizontal-loop controlled source electromagnetic inversion method and its use to characterize heterogeneity in aquiferous fractured crystalline rocks, *Geophys. J. Int.*, **166**, 59-66.
- Won, I.J., 2003, Small frequency-domain electromagnetic induction sensors, *The Leading Edge*, **22**, 320-322.